IET Optoelectronics

Special Issue on Optical-Wireless Communications

IET Journals
The Institution of Engineering and Technology

Performance evaluation of wireless optical communication for mobile body area network scenario with blocking effects

ISSN 1751-8768
Received on 4th November 2014
Revised on 24th April 2015
Accepted on 2nd June 2015
doi: 10.1049/iet-opt.2014.0145
www.ietdl.org

Ludovic Chevalier ✉, *Stephanie Sahuguede*, *Anne Julien-Vergonjanne*

XLIM DPT-C2S2 UMR CNRS 7252/LABEX Sigma-Lim, University of Limoges, France
✉ *E-mail: Ludovic.chevalier@ensil.unilim.fr*

Abstract: Using wireless optical communication (WOC) to establish on-body links constitutes a promising solution to address radiofrequency interference issues in body area network (BAN) especially concerning medical applications. Actually, this permits decreasing electromagnetic perturbations in the patient body environment. To evaluate WOC performance for BAN scenario, the authors investigate on-body communication between a BAN node and the central unit placed on the patient which is supposed to be moving in a room. Considering a diffuse optical transmission scheme based on optical reflections over the environment, the authors propose an adapted, fast and simple method to determine the performance taking into account the presence of obstacles in the room. Thanks to this method, the authors evaluate the WOC outage probability assuming uniform node mobility on the patient body and patient mobility in the environment. The results permit discussing the WOC robustness according to the optical reflection properties of the blocking elements and show the WOC potentialities for mobile medical BAN scenario.

1 Introduction

Body area network (BAN) is a recent and promising technology at the human scale which enables wireless communications between sensors and a central unit generally placed on the body [1]. This central unit is the coordinator node establishing wireless connections with all BAN devices but also with other networks in the environment. One main BAN application is in the field of e-health because these networks could provide continuous remote monitoring and thus early detection of abnormal patient health conditions. In medical context, there are many specifications in terms of reliability and latency but also in terms of power consumption which has to be low in order to achieve a long lifetime network [2].

In this context and considering on-body sensors, the wireless link between a sensor and the central unit placed on the patient body has thus to be robust and efficient even if the patient is moving. For this purpose, radiofrequency technology (RF) in ultra wide band is generally used because of the low power spectrum density and high capacity of transmission it offers [3–5]. However, recent studies [6] show that the electromagnetic interferences of RF devices over medical equipment could be critical. Moreover, the effect of a long RF exposure on health is still undetermined. Thus, to avoid the increase of RF links in the patient environment, alternative solutions such as wireless optical communication (WOC) are investigated. For indoor applications, WOCs have been recently an active field of research thanks to their immunity toward RF ones, but also for the increase in the high data rates demand and the safe data transfer they provide [7–18]. In particular, for mobile health monitoring applications, previous studies have explored the performance of WOC between a central unit placed on a patient and a base station fixed in the indoor environment [13, 15]. We propose here to enlarge these investigations to the field of mobile BAN, by evaluating the performance of an on-body link using WOC.

Different schemes of WOC can be used, according to the alignment requirements of optical devices [16]. The most performing one is the line of sight (LOS) which corresponds to a direct path with a perfect alignment between the transmitter and the receiver. However, LOS scheme is not adapted to BAN scenario because it is difficult to establish a direct link between two body nodes considering the variety of human body morphologies. Consequently, we study a non-LOS scheme exploiting diffuse optical reflections over the environment. We have already investigated a static monitoring scenario where a sensor placed on a patient lying on a bed transmits data to the BAN coordinator by using diffuse optical transmission [14].

In this paper, the patient is assumed to be moving within a hospital room including obstacles. Several studies have been already published on shadowing and blocking effects in indoor WOC [17, 18], however they do not address BAN scenario. Our contribution is to develop a simple approach to determine the impact of an obstacle on the performance of mobile BAN. For this purpose, we propose an adaptation of the well-known one-bounce model [8] for diffuse propagation to the case where an obstacle is in front of the BAN. This adapted method permits a lower time consuming study than classical numerical solutions such as ray-tracing techniques [19].

The paper is organised as follows. Section 2 describes the studied system and the BAN scenario. The different existing models to simulate the optical channel and the solution used to evaluate the impact of an obstacle are presented in Section 3. Section 4 presents and discusses the performance results obtained by simulation before concluding in Section 5.

2 System description

The studied environment is a typical hospital room of dimensions (3, 4, and 2.5 m) as shown in Fig. 1*a*. A patient equipped with sensors is supposed to be moving in the room. To take into account this mobility, we use a two-dimensional uniform distribution of the patient positions (x_p, y_p). An obstacle is assumed to be centred at $x_{obs} = 1.5$ m and $y_{obs} = 2$ m, with a height of 1.70 m and a width of 0.5 m as presented in Fig. 1*a*. These dimensions have been chosen so as the obstacle could be the body of another person present in the room for example. An infrared (IR) transmitter coupled with a sensor located on the patient body is communicating with a central unit device so-called hub. In addition, as we investigate BAN scenario, we suppose that the hub position is fixed on the patient

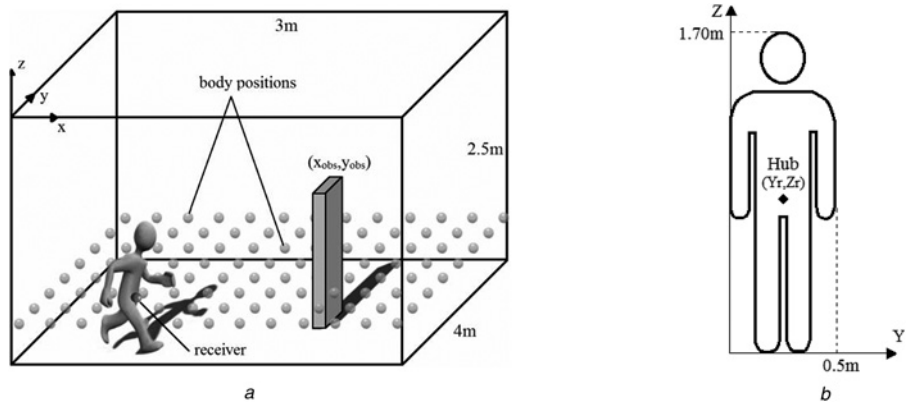

Fig. 1 *Studied indoor environment (a), and patient body (b)*

body, whereas the transmitter can be placed at any positions, uniformly distributed on the body. The hub is located at the waist as shown in Fig. 1*b*, at $Y_r = 0.25$ m, and $Z_r = 1$ m considering the patient viewpoint. Moreover, the transmitter and the hub are supposed to be in the same plane, and oriented so as to be perpendicular to the patient body. This permits assuming in a first approach, that the patient body has no impact on the optical link.

Besides, data are sent using intensity modulation and direct detection (IM/DD). Thus, the signal received by the photo-detector at the hub depends on the incident optical power and the photo-detector responsivity R. An IR channel with IM/DD can be modelled by a linear system [8] and the received signal $y(t)$ is thus written as:

$$y(t) = R \times x(t) \otimes h(t) + n(t) \tag{1}$$

where $x(t)$ is the transmitted signal, $h(t)$ represents the impulse response of the optical channel, and $n(t)$ is an additive white Gaussian noise.

For health monitoring applications, the maximal data-rate is generally around 1 Mb/s [20, 21]. Thus, according to previous works [8], the inter-symbol interference can be neglected and the impulse response can be only characterised by its static gain H_0

$$h(t) = H_0 \times \delta(t) \tag{2}$$

In the case of diffuse transmissions, the node corresponding to the emitter projects an optical beam on the environment surfaces including obstacle surface. Then, the reflected signals are collected by the optical receiver at the hub. Assuming both variations of the transmitter position on the patient body and of the patient position in the room, the optical gain value H_0 randomly varies. To determine the distribution of H_0 considering the presence of an obstacle, we develop in the next section a fast and simple way derived from one-bounce model [8]. For this purpose, we assume in a first approach that the two communication nodes are directed towards the obstacle. In addition, the transmission node is considered in the following having a Lambertian emission.

3 Channel model

3.1 One-bounce model

A well suited model to describe diffuse transmissions is the so called one-bounce model [8]. Thanks to this model, it is possible to calculate the optical gain H_0 between the transmitter and the receiver considering one reflection per optical beams. To apply this model to the studied scenario, we define five surfaces S_n in the indoor environment, with n varying between 1 and 5, as presented in Fig. 2.

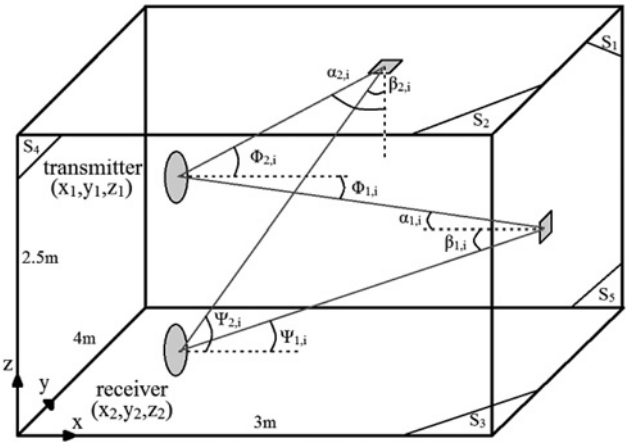

Fig. 2 *One-bounce model description*

Each radiated beam from the transmitter is reflected by the small parts of S_n contained in the field of view (FOV) of the receiver. The total received power is then the sum of the contributions from all the tiny elements dS_n of the reflective surface S_n. The optical gain H_{0,S_n} corresponding to the reflective surface S_n is expressed as [8]:

$$H_{0,S_n}(\rho_n) = \frac{A\rho_n}{\pi^2} \iint_{S_n} \frac{\cos(\Phi_{n,i})\cos(\alpha_{n,i})\cos(\beta_{n,i})\cos(\Psi_{n,i})}{d_{n,i,1}^2 d_{n,i,2}^2} dS_n \tag{3}$$

where ρ_n is the surface reflection coefficient which can take values between 0 and 1, A represents the physical surface of the photo-detector, $d_{n,i,1}$ the distance between the transmitter and the surface element of S_n, $d_{n,i,2}$ the distance between the receiver and the surface element of S_n. The angles ($\beta_{n,i}$, $\alpha_{n,i}$, $\Phi_{n,i}$, $\Psi_{n,i}$) are defined in Fig. 2 for each tiny elements dS_n of the reflective surface. Using (3), the optical gain considering all the surfaces S_n can be thus obtained from:

$$H_0 = \sum_{n=1}^{5} H_{0,S_n}(\rho_n) \tag{4}$$

In our configuration we have supposed that the BAN nodes are directed toward S_1. This is a simplification meaning that rotations of the patient body are not taken into account. Thus, the main reflective surface, that is, the one which contributes the more to the optical gain H_0, is supposed to be S_1.

To verify this statement, the optical gain and delay spread distributions are calculated using (3) and (4), for the room free of

IET Optoelectron., 2015, Vol. 9, Iss. 5, pp. 211–217

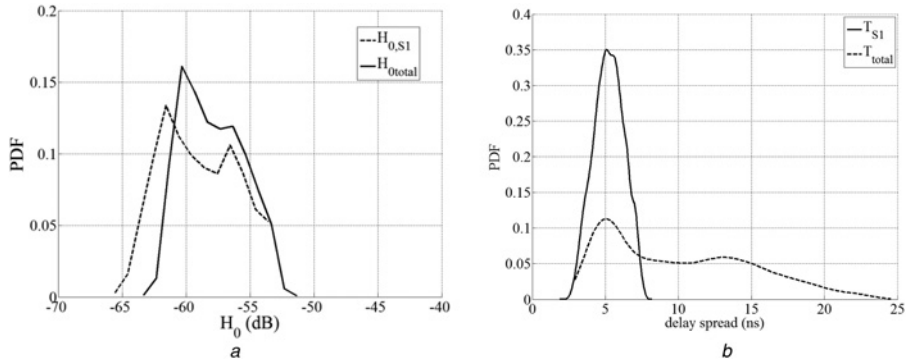

Fig. 3 *Optical gain (a) and impulse response length (b) distributions in the empty room*

any obstacle. We have performed calculation considering one thousand possible positions of the patient body in the room and one hundred positions of the transmitter on the patient body.

The results provided in Fig. 3*a* represent the optical gain distributions of H_{0,S_1} and $H_{0\text{total}}$. H_{0,S_1} is the optical gain calculated using (3), considering only the main surface S_1. $H_{0\text{total}}$ is the optical gain calculated using (4), considering all the reflective surfaces. All the reflection coefficients have been set to 0.8 [8]. We can observe that the two distributions are close which confirms that for the described scenario, the reflective surface S_1 is the most contributing one.

The results provided in Fig. 3*b* represent the delay spread distribution. In plain lines we have reported the one (T_{S_1}) obtained using the values of $d_{n,i,1}$ and $d_{n,i,2}$ from (3), considering only the main surface S_1, and in dotted lines the one corresponding to the total impulse response length (T_{total}) considering all the reflective surfaces. It can be noted that the most occurring value is the same for each distribution, that is, 5 ns. Moreover, compared with T_{S_1}, the distribution of T_{total} presents higher values of delay spread (up to 25 ns instead of 8 ns), due to the higher number of reflective surfaces. However, in our study, we consider low data rate values required for health monitoring (<1 Mb/s) [20, 21]. Thus, the underestimation of the delay spread made by considering only the surface S_1 will not affect our study. Thus, these results permit simplifying the gain calculation approach and we only take into account the contribution of S_1 called S_{main} in the following.

3.2 Adapted one-bounce model

Considering now the presence of an obstacle in the room, as defined in Fig. 1, we have adapted the one bounce model for the gain calculation. An obstacle can be represented by a surface S_{obs} situated between the node plane and the reflective surface S_{main} (see Fig. 4).

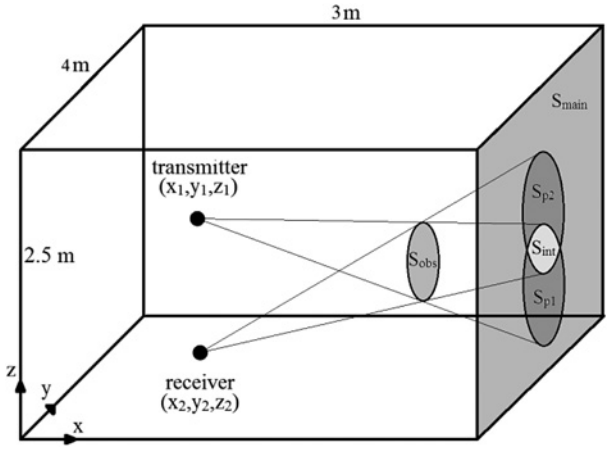

Fig. 4 *Adapted one-bounce model description*

The surface S_{obs} can disrupt the diffuse link between the transmitter and the receiver. Thus, we first determine the projection of S_{obs} on the wall from the transmitter and the receiver. The resulting surfaces S_{p1} and S_{p2} are parts of the main surface, S_{main}, which cannot contribute anymore to the communication between the two nodes. If an intersection surface named S_{int} between these two surfaces exists, it has to be taken into account to calculate the whole optical gain. The value of the optical gain $H_{0\text{adapted}}$, taking into account the presence of the obstacle can be obtained from:

$$H_{0\text{adapted}} = H_{S_{\text{main}}} + H_{S_{\text{obs}}} - H_{\text{lost}} \tag{5}$$

where $H_{S_{\text{main}}}$ is the optical gain provided by the entire wall surface, $H_{S_{\text{obs}}}$ is the one provided by the obstacle surface S_{obs}, and H_{lost} corresponds to the gain part lost from the surface elements of the wall (S_{p1}, S_{p2}, S_{int}). Thus, H_{lost} can be written as:

$$H_{\text{lost}} = H_{S_{p1}} + H_{S_{p2}} - H_{S_{\text{int}}} \tag{6}$$

Each of the terms in (5) and (6) can be calculated using (3)

$$H_{S_{\text{main}}} = H_{0,S_{\text{main}}}(\rho) \tag{7}$$

$$H_{S_{\text{obs}}} = H_{0,S_{\text{obs}}}(\rho_{\text{obs}}) \tag{8}$$

$$H_{S_{p1}} = H_{0,S_{p1}}(\rho) \tag{9}$$

$$H_{S_{p2}} = H_{0,S_{p2}}(\rho) \tag{10}$$

$$H_{S_{\text{int}}} = H_{0,S_{\text{int}}}(\rho) \tag{11}$$

ρ is the wall reflection coefficient and ρ_{obs} is the obstacle surface reflection coefficient. The term $H_{S_{\text{int}}}$ is subtracted to H_{lost} to ensure that the intersection surface S_{int} is taken into account only once.

3.3 Adapted one-bounce model validation

To validate our adapted model, we have used a ray-based simulator developed at the XLIM Laboratory named RapSor [19]. It offers the possibility to simulate the propagation of a wave according to several physical configurations from the hypothesis of high frequency approximation. It is based on techniques such as a classical ray launching associated to Monte Carlo algorithm.

For an obstacle defined as in Fig. 1, the optical gain and delay spread distributions obtained by using RapSor ($H_{0\text{RapSor}}$, T_{rapsor}), and by using the adapted model ($H_{0\text{adapted}}$, T_{adapted}) are reported in Figs. 5*a* and *b*. They have been calculated using the following configuration, assuming one reflection per optical beam:

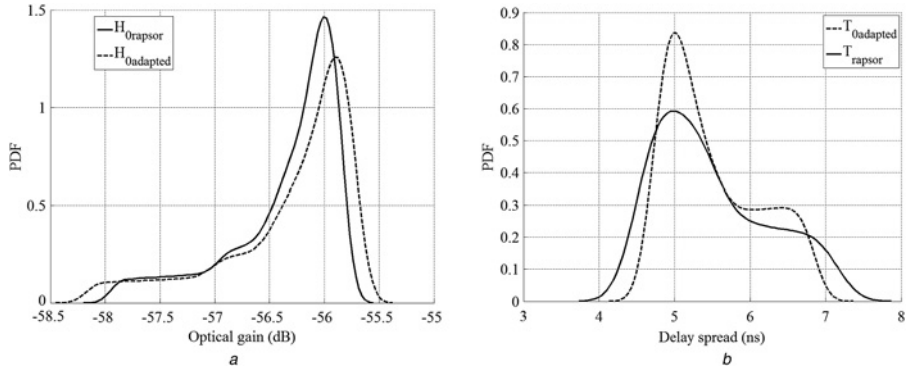

Fig. 5 *Adapted one-bounce model validation in terms of optical gain (a) and in terms of delay spread (b)*

- One patient body position fixed at $x_p = 1$ m, and $y_p = 2$ m is considered.
- The receiver position is fixed on the body as shown in Fig. 1*b*.
- One thousand transmitter positions are uniformly distributed on the patient body.
- The rectangular obstacle surface is centred at $x_{obs} = 1.5$ m and $y_{obs} = 2$ m, with a height of 1.70 m and a width of 0.5 m.
- Reflection coefficients are all set to $\rho = \rho_{obs} = 0.8$.

We can observe that the two gain distributions presented in Fig. 5*a* are close. In addition, the two impulse response length distributions shown in Fig. 5*b* provide similar results, with the same mean value of 5 ns. Thus, this permits validating the use of the adapted one-bounce model as a suitable alternative to ray-tracing methods when one reflection per optical beam is considered. For a number of reflections set to three [8], the ray-tracing computation of the same configuration provides the results shown in Figs. 6*a* and *b*.

We can observe in Fig. 6*a* that the optical gain distribution obtained with three reflections per optical beam has a similar shape as the one obtained with one reflection, but translated by about 3.5 dB with a width 0.5 dB shorter. The gain distribution characteristics are different but it can be noted that results regarding probability calculations are similar. For example, the probabilities of having an optical gain lower than its mean value, that is, −56.8 dB for the one-reflection approximation and −52.8 dB for the three-reflections analysis, are about 35% in both one- and three-reflections studies. Thus, it will be valid to use the proposed model regarding the impact of obstacles in terms of performance variations, thanks to all the simplifications we made:

- Low data rates (<1 Mb/s).
- Inter-symbol interference neglected.
- One reflection per optical beams.
- Communication nodes always directed towards the wall in front of the patient body.
- The wall in front of the patient body is the main contributing one.

The main drawback due to this simplified model is an overestimation of the required transmitting power to achieve a robust link. To continue, the results presented in Fig. 6*b* show the impact of the multiple reflections on the delay spread. The responses are about seven times longer in the three reflection case than in the single reflection one. For example, the difference in terms of mean value is about 32 ns. As in our study, we consider low data rate values required for health monitoring (<1 Mb/s) [20, 21], this difference will not impact our conclusions regarding obstacle impact.

Thus, we will use the proposed model assuming one reflection per beam. Actually, the calculation time required for simulation for one body position with the adapted model is about 20 times faster than with ray-tracing software such as RapSor. This constitutes a great advantage considering patient mobility that involves a calculation for a high number of patient body positions in the room. This is the main reason for using the adapted model in the following to determine the wireless optical on-body communication performance variations because of the presence of obstacles.

4 Performance results

4.1 Outage probability

In the mobile BAN scenario, we consider node mobility on the patient and patient movements in the room. This double mobility induces random variations of optical gain. However these variations are slow even for the low data rates required for health monitoring (<1 Mb/s) [20, 21]. So, in the following, we study performance by determining the outage probability instead of the bit error rate (BER), which does not represent in this case a good

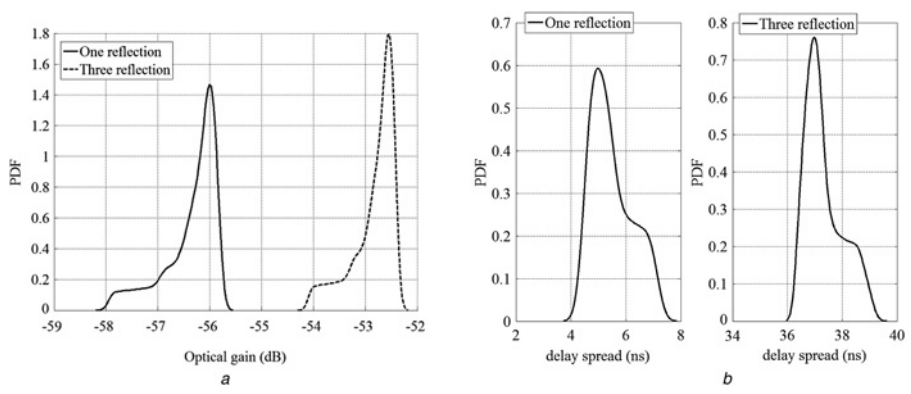

Fig. 6 *Optical gain (a) and impulse response length (b) with one and three reflections*

IET Optoelectron., 2015, Vol. 9, Iss. 5, pp. 211–217

metric [13]. The outage probability can be expressed as the probability that the signal to noise ratio (SNR) value drops below a threshold SNR_0 [22]

$$P_{out}(SNR_0) = P_r(SNR < SNR_0) \quad (12)$$

For on–off keying (OOK) modulation the received SNR can be defined as [13]:

$$SNR = \frac{2R^2 H_{0adapted}^2 P_t^2}{D_b N_0} \quad (13)$$

with N_0 the noise power spectral density, D_b the data rate, and P_t the transmitted optical power.

In this study, we consider transmissions at an optical wavelength of 875 nm for which standards define a maximum radiated intensity of 95.5 mW/sr [23]. For a half-power transmitter angle of 60°, the maximum transmission power is $P_t = 300$ mW. In the context of health monitoring we consider a data rate D_b of 1 Mb/s. The receiver has a FOV of 70°, a responsivity $R = 0.55$ A/W and a physical surface A of 1 cm^2. Moreover we consider a classical noise power spectral density value of $N_0 = 6.4 \times 10^{-23}$ W/Hz [7].

First, we investigate the outage probability performance assuming one obstacle in the environment, as shown in Fig. 1*a* and compare the results to the case of an empty room.

4.2 Performance with a fixed obstacle

As in part 3-C, the obstacle is modelled by a rectangular surface with reflection coefficient ρ_{obs} and is centred at $x_{obs} = 1.5$ m and $y_{obs} = 2$ m, with a height of 1.70 m and a width of 0.5 m. In addition, one hundred transmitter node positions are uniformly and randomly distributed over the body. The receiver node on the patient body is fixed at $Y_r = 0.25$, and $Z_r = 1$ m. Moreover, the patient body positions are now uniformly and randomly distributed in the room as illustrated in Fig. 1*a*. One thousand body positions have been defined. Then, the outage probability P_{out} is determined from the SNR distribution obtained using (13), thanks to the adapted one-bounce model we have developed for the optical gain calculation.

On Fig. 7, we have reported the outage probability obtained considering the environment with and without the obstacle and for different transmission power values P_t. Besides, the performances have been evaluated for a wall reflection coefficient of $\rho = 0.8$, and two extreme values of obstacle reflection coefficients ρ_{obs} (0.2;0.8).

As expected, we can see that the outage probability can be reduced by decreasing the targeted SNR_0 value, and by increasing the transmission power.

Health monitoring applications generally require a high reliability corresponding to low BERs. Hence, we consider in the following a minimal BER of 10^{-9} with an OOK modulation. This corresponds to a targeted SNR_0 of 15.6 dB.

Considering an outage probability of 10^{-3}, we can deduce from the results that the minimal transmission power needed in order to achieve the required SNR_0 is $P_{tmin} = 180$ mW which is much lower than the maximal permitted power for diffuse transmission ($P_{tMax} = 300$ mW). Moreover, it can be noted that these results have been obtained from simplified model considering only one reflection over one surface and on the obstacle. Thus, the P_{tmin} value is overestimated and represents the worst possible estimation. For example, for one patient body position in the centre of the empty room, we have used ray-tracing method (RapSor) considering three reflections per optical beams. For the same targeted values of P_{out} and SNR_0, the minimal transmission power value is 13 mW, which is much lower than the value of 180 mW obtained with the proposed model. As we have said previously, this shows that this model has to be used for evaluating the impact of obstacles, but at the cost of transmission power overestimation.

In addition, we can verify from Fig. 7 that the performance is not highly affected by blocking effect of obstacle surface, and this whatever the obstacle reflection coefficient. This is even truer that the targeted P_{out} is low, and can be explained because of two reasons. First, regarding the uniform distribution of the body positions and the obstacle position (x_{obs}, y_{obs}), most of the time the obstacle is not directly in front of the patient. Then, the size of the obstacle considered for the results presented in Fig. 7 is too small to provide a significant impact on the performance with such patient mobility. To evaluate the obstacle size impact, we have plotted in Fig. 8 the SNR_0 corresponding to a P_{out} of 10^{-3} as a function of the obstacle width for $P_t = 180$ mW and for different values of ρ_{obs}.

As expected, increasing the size of the obstacle induces a significant impact on the performance. In addition, it can be noted that depending on the value of ρ_{obs}, the presence of the obstacle can improve or not the performance. For example, regarding the SNR_0 value of 15.6 dB for a small size obstacle, an obstacle of 1.5 m width increases the SNR_0 value of 11% if $\rho_{obs} = 0.8$. However, if $\rho_{obs} = 0.2$, we can observe a decrease in the SNR_0 value of 15.5%.

Whatever the obstacle width and for the defined obstacle position, the minimal value of ρ_{obs} which permits improving the SNR_0 compared with the empty room case, is $\rho_{obsmin} = 0.27$. This result shows that even with a low reflection coefficient, an obstacle could tend to contribute to the transmission. Regarding the classical value of $\rho = 0.8$ generally considered in IR communications [8], the value of ρ_{obsmin} is significantly lower. This shows the potential of diffuse transmissions for on-body communications. However,

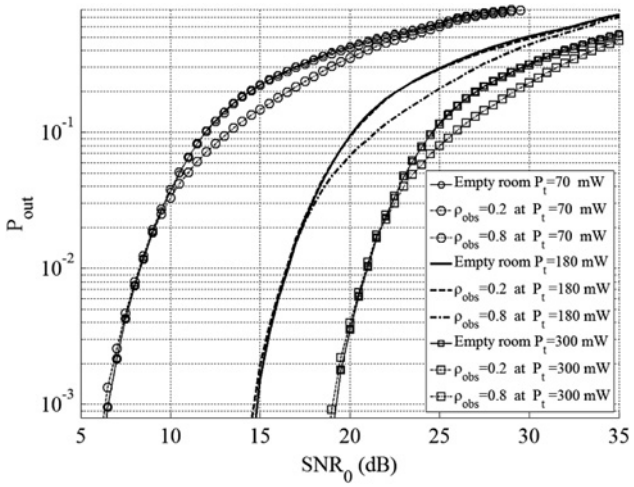

Fig. 7 *Simulation results for one obstacle*

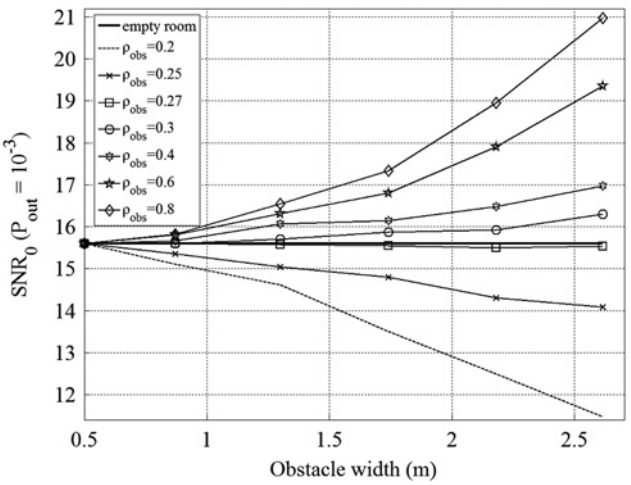

Fig. 8 *Impact of the obstacle size*

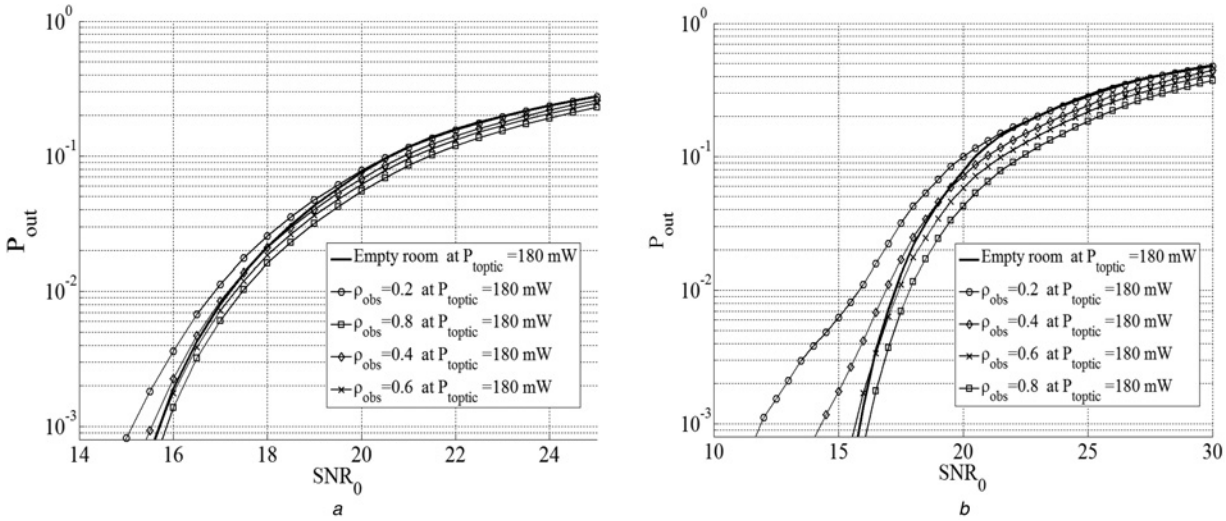

Fig. 9 *Impact of the obstacle mobility with a width of 0.5 m (a) and of 1.5 m (b)*

these results are based on a motionless obstacle. Thus, in the next part, we investigate the impact of the mobility of the obstacle in addition to the patient one.

4.3 Performance with obstacle mobility

We consider now a two dimensional uniform distribution of the obstacle positions (x_{obs}, y_{obs}), in the room presented in Fig. 1*a*. The reflection coefficient of the room walls is $\rho = 0.8$ and the obstacle height is of 1.70 m. The corresponding P_{out} is plotted in Fig. 9 as a function of SNR_0, for different values of ρ_{obs} and for two extreme values of the obstacle width (0.5 m; 1,5 m), which could respectively correspond for example to another person or a fully equipped medical trolley.

Regarding the case of an obstacle width of 0.5 m (Fig. 9*a*), we can remark here that the obstacle mobility induces small variations of the SNR_0 values for $P_{out} = 10^{-3}$, depending on the value of ρ_{obs}, which had no impact when the obstacle was motionless. For example, if $\rho_{obs} = 0.2$, the performance is slightly degraded as SNR_0 is 0.6 dB lower than in the empty room case, whereas if $\rho_{obs} = 0.8$, the performance is quite the same as SNR_0 is 0.1 dB higher. These SNR_0 variations are still low because of the small size of the obstacle. Regarding a higher obstacle width of 1.5 m (Fig. 9*b*), the performance can be more significantly impacted as the SNR_0 is 4 dB lower than the empty room case for $\rho_{obs} = 0.2$, whereas for $\rho_{obs} = 0.8$, the SNR_0 is 0.3 dB higher.

If we search the minimal ρ_{obs} value corresponding to performance improvement, we obtain here $\rho_{obsmin} = 0.6$. This result is different from the previous case considering a motionless obstacle and shows that the obstacle position in the environment has to be considered to evaluate its impact on the performance.

Besides, we can see that the performance improvement regarding high values of ρ_{obs} is not enough significant to be considered as an advantage, whereas the decrease in performance for low values of ρ_{obs} cannot be neglected.

Finally, the simplified approach we have proposed permits assessing with reduced time computation, the impact of obstacles taking into account their position, size and reflection coefficient.

5 Conclusion

In this paper we have investigated wireless optical on-body communication between a medical BAN node and the central unit placed on the patient body considering blocking effect because of an obstacle in the environment. We have taken into account the mobility of the BAN emitter node on the patient body and the patient mobility within the environment. To establish the mobile on-body link, a diffuse optical transmission scheme based on optical reflections over the environment has been studied.

To assess the impact on the performance due to the presence of an obstacle in the environment, we have proposed a simple way, adapted from the one-bounce model to evaluate the static gain of the mobile wireless optical channel. This approach provides results with a much lower computation time than using numerical methods such as ray-tracing technique and permits performing parametric study of the obstacle impact, especially regarding size, position and reflectivity characteristics.

The results presented in this paper show that one obstacle of dimensions close to patient body ones, does not significantly impact WOC performance for mobile medical BAN scenario with data rates lower than 1Mbps and requiring low BER. However, increasing obstacle size or taking into account its mobility leads to significant variations of the performances in terms of outage probability. These variations can benefit or spoil the transmission, depending on the reflection coefficient of the obstacle. This means that a complete knowledge of the optical property of room elements is important for design issue.

Finally, this study illustrates the potentiality of diffuse WOC to establish on-body links. It permits investigating in a future work the performance of several wireless optical on-body links in a BAN, constituting a promising alternative to radiofrequencies for medical applications.

6 References

1 IEEE 802.15.6 standard for Local and metropolitan area networks—Part 15.6: Wireless Body Area Networks, 2012

2 Tar'in, C., Traver, L., Cardona, N.: 'Wireless body area networks for telemedicine applications', *Mag. Waves*, 2009, pp. 124–125

3 Di Benedetto, M.-G., Kaiser, T., Molisch, A.F., Opperman, I., Politano, C., Porcino, D.: 'UWB communication systems, a comprehensive overview', 2006, pp. 3–8, ISBN 977-5945-10-0

4 Hämäläinen, M., Taparugssanagorn, A., Iinatti, J.: 'On the WBAN channel modelling for medical applications'. European Conf. on Antennas and Propagation (EUCAP), 2011, pp. 2967–2971

5 Cheffena, M.: 'Time-varying on-body wireless channel model during walking', *EURASIP J. Wirel. Commun. Netw.*, 2014, **29**, doi: 10.1186/1687-1499-2014-29

6 Periyasam, M., Dhanasekaran, R.: 'Electromagnetic interference on critical medical equipment by RF devices'. Int. Conf. on Communications and Signal Processing (ICCSP), 3–5 April 2013, pp. 78–82

7 Gfeller, F., Bapst, U.: 'Wireless in-house data communication via diffuse infrared radiation', *Proc. IEEE*, 1979, **67**, (11), pp. 1474–1486

8 Kahn, J.M., Barry, J.R.: 'Wireless infrared communications', *Proc. IEEE*, 1997, **85**, (2), pp. 265–298

9 Carruthers, J.B.: 'Wireless infrared communications' (Wiley Encyclopedia of telecommunications, New York, 2003)

10 Borah, K., Boucouvalas, A.C., Davis, C.C., Hranilovic, S., Yiannopoulos, K.: 'A review of communication-oriented optical wireless systems', *EURASIP J. Wirel. Commun. Netw.*, **91**, doi: 10.1186/1687-1499-2012-91
11 Fadlullah, J., Kavehrad, M.: 'Indoor high-bandwidth optical wireless links for sensor networks', *J. Lightw. Technol.*, 2010, **28**, (21)
12 Elgala, H., Mesleh, R., Haas, H.: 'Indoor optical wireless communication: potential and state-of-the-art', *IEEE Commun. Mag.*, 2011, **49**, (9), pp. 56–62, doi: 10.1109/MCOM.2011.6011734
13 Torkestani, S.S., Barbot, N., Sahuguede, S., Julien-Vergonjanne, A., Cances, J.P.: 'Performance and transmission power bound analysis for optical wireless based mobile healthcare applications'. IEEE 22nd Int. Symp. on Personal Indoor and Mobile Radio Communications (PIMRC), 2011, pp. 2198–2202
14 Chevalier, L., Sahuguede, S., Julien-Vergonjanne, A., Combeau, P., Aveneau, L.: 'Investigation of wireless optical technology for communication between on-body nodes'. Second Int. Workshop on Optical Wireless, 2013
15 Torkestani, S.S., Sahuguede, S., Julien-Vergonjanne, A., Cances, J.P.: 'Indoor optical wireless system dedicated to healthcare application in a hospital', *IET Commun.*, 2012, **6**, (5), pp. 541–547
16 Ghassemloy, Z., Popoola, W., Rajbhandari, S.: 'Optical wireless communications, system and channel modeling with MATLAB®', 2013, pp. 11–18, ISBN 978-1-4398-5188-3
17 Jivkova, S., Kavehrad, M.: 'Shadowing and blockage in indoor optical wireless communications'. IEEE Proc. Global Telecommunications Conf., 2003, pp. 3269–3273
18 Komine, T., Haruyama, S., Nakagawa, M.: 'A study of shadowing on indoor visible-light wireless communication utilizing plural LED lightings', *Wirel. Pers. Commun.*, 2005, **34**, (1–2), pp. 211–225
19 Behlouli, A., Combeau, P., Aveneau, L., Sahuguède, S., Julien-Vergonjanne, A.: 'Efficient simulation of optical wireless channel, application to WBANs with MISO link', *Procedia Comput. Sci.*, 2014, **40**, pp. 190–197, ISSN 1877-0509, http://dx.doi.org/10.1016/j.procs.2014.12.027
20 Paksuniemi, M., Sorvoja, H., Alasaarela, E., Myllyla, R.: 'Wireless sensor and data transmission needs and technologies for patient monitoring in the operating room and intensive care unit'. 27th Annual Int. Conf. of the Engineering in Medicine and Biology Society, 2005, pp. 5182–5185
21 Movassaghi, S., Abolhasan, M., Lipman, J., Smith, D., Jamalipour, A.: 'Wireless body area network: a survey', *IEEE Commun. Surv. Tutor.*, 2014, (99), pp. 1–29, doi: 10.1109/SURV.2013.121313.00064
22 Goldsmith, A.: 'Wireless communications' (Cambridge UnivPr, 2005)
23 IEC 60825-1: 'safety of laser products-part 1: equipment classification, requirements, and user's guide', 2001, 1.2 Edition.L